Processive hand-over-hand motion of homodimeric nanomotors induced by interaction between two monomeric components and thermal noise

Ping Xie*

Laboratory of Soft Matter Physics, Institute of Physics, Chinese Academy of Sciences, Beijing 100190, China

(Received 23 July 2008; revised manuscript received 28 November 2008; published 27 January 2009)

A simple homodimeric nanowalker is presented that is capable of moving processively along an extended periodic track. The unidirectional motion is based on a mechanism that makes use of the interaction between the two monomers and the thermal noise. The effect of the neck linker, which plays a critical role in the previously proposed design, plays an unimportant role in the present system. Except the requirement of a fixed binding orientation of the monomer relative to the track at the minimum of the potential well, the system has no other requirement for the form of the interaction potential between the motor and the track, which is critical to the unidirectional movement of the monomeric motor. Using detailed analyses and numerical simulations, it is shown that the homodimeric nanowalker walks hand over hand along the track with a high efficiency and a high stall force.

DOI: 10.1103/PhysRevE.79.011920 PACS number(s): 87.85.Qr, 84.60.Bk, 05.40.−a

I. INTRODUCTION

Molecular motors or nanomachines have attracted considerable interest both theoretically and experimentally because of potential nanotechnological applications [1–10]. An important class of the molecular motors is the one that can move directionally along an extended track [11–20], thus making it possible to precisely transport a nanoscale object from one location on the nanometer-wide track to another location along a designed path. A simple and well-studied molecular motor of this class is the monomeric molecule that moves unidirectionally by making use of the Brownian ratchet mechanism [11–13]. Generally, two types of ratchet models have been proposed. One is the fluctuating-force ratchet, i.e., the particle is subject to an external unbiased driving force [21–23]. The other one is the fluctuating-potential ratchet, i.e., the particle feels a fluctuating potential between on and off [24,25]. However, the molecular motor by making use of this mechanism usually possesses a low efficiency, a low stall force, and a low processivity.

Recently, inspired largely by discoveries of biological dimeric kinesin motor proteins that make intracellular vesicle transportations [26–28], a lot of effort has been made in the design and fabrication of dimeric nanowalkers that can walk directionally along the extended track [14,15,29–31]. One design was made by simply coupling two identical particles harmonically, each of which moves in a common potential via the ratchet mechanism of single particles [29,30]. The synthetic dimeric nanowalkers reported up to now are heterodimers and the track contains multiple species of anchorages in an ordered arrangement [14,15]. Moreover, multiple species of fuel reagents are required for forming and breaking of different types of foot-anchorage binding combinations and temporally ordered consumption of different reagent species. These are nearly the highest requirements for motor-track systems.

More recently, Wang proposed a design of a relatively simple bipedal nanowalker that can move hand over hand along the extended periodic track, with the walker having a pair of identical pedal components connected by a polymer chain [31]. The design has the following requirements. In the vicinity of a foot-anchorage binding combination, the adjacent polymer is partially straightened and aligned toward a unique end of the array of anchorages. The polymer alignment must be disrupted after the foot is detached from the track. The interactions enabling the alignment also must modulate the overall affinity of the foot with the track so that a technical means can be developed for discriminately detaching an alignment-associated foot rather than an alignment-free one. Thus, in this walker-track system, the alignment-pointed direction of the adjacent polymer determines the direction of the walker. The idea for this design of the nanowalker is more similar to that used in the proposed models for the dimeric kinesin, where the docking of the neck liner plays the critical role in the forward stepping of the detached trailing head [32,33].

In this work, we propose a simple system of homodimeric nanowalker and track. The unidirectional motion of the walker along the track is based on a mechanism that makes use of the interaction between the two identical monomers and the thermal noise. The proposal is mainly inspired by the moving mechanism of the dimeric kinesin along a microtubule, which was proposed recently by us [34–37]. By detailed analyses and calculations it is shown that the dimeric nanowalker can walk hand over hand along the periodic track with a high efficiency, a high velocity, and a high stall force.

II. WALKER-TRACK SYSTEM

The system we propose is composed of a walker and a track. The walker consists of two identical monomers. Each monomer is connected by a polymer chain that is called the neck linker and the two neck linkers are connected together on their other ends. The track has an extended structure with a periodic array of binding sites for the monomer. For this system, we have three kinds of interactions, i.e., (i) the interaction between two monomers of the walker, (ii) the interac-

*pxie@aphy.iphy.ac.cn

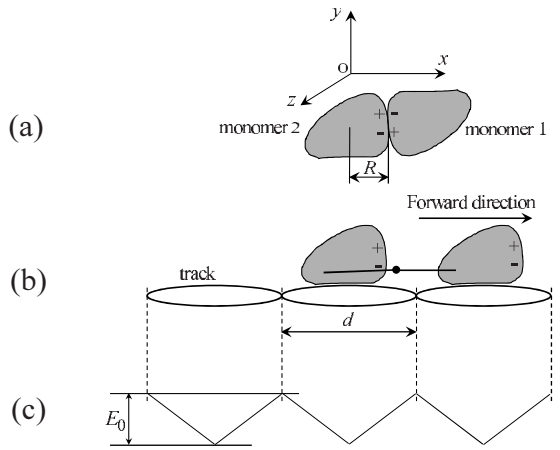

FIG. 1. Conformations of the homodimeric nanowalker in free state (a) and in rigor state (b). Two monomers of the walker interact with each other via electrostatic force. Symbols "+" and "−" represent positive and negative charges, respectively. (c) Interaction potential $V_S^{(x)}(x)$ of a monomer with the track along the x direction.

tion between the neck linker and the monomer, and (iii) the interaction between the monomer and the track. The three kinds of interactions are described as follows.

The two monomers interact with each other via electrostatic force, as schematically shown in Fig. 1(a). Based on the Debye-Huckel theory, the electrostatic potential in solution can be quantitatively described in the form

$$V_{M-M}(x,y,z) = -V_0 \exp(-\sqrt{(x-x_1)^2+(y-y_1)^2+(z-z_1)^2}/A_r). \quad (1)$$

Here, (x,y,z) is the center-of-mass coordinate of one monomer (monomer 1) relative to that of the other monomer (monomer 2), with the center-of-mass position of monomer 2 being taken as the origin of the coordinate [see Fig. 1(a)]; (x_1,y_1,z_1) is the center-of-mass position of monomer 1 where it has the strongest interaction with monomer 2, corresponding to the equilibrium conformation of the dimer; $V_0>0$ is the interaction strength; and A_r is the Debye length. Denoting the distance between the center-of-mass position of one monomer and its interacting site with another monomer as R [see Fig. 1(a)], we have $(x_1,y_1,z_1)=(2R,0,0)$. It is pointed out here that the interaction V_{M-M} between two monomers is not varied with time, independent of the external operation or stimulus that modulates the interaction between the monomer and the track (see below).

The neck linker is considered to be capable of rotating freely around its jointing point to the monomer. Moreover, the neck linker can be stretched elastically, with the elastic force being written as

$$F_{NL}(r) = C(r-r_0), \quad \text{when } r > r_0, \quad (2a)$$

$$F_{NL}(r) = 0, \quad \text{when } r \leqslant r_0, \quad (2b)$$

where C is the elastic coefficient, $r \equiv \sqrt{x^2+y^2+z^2}$ is the distance between two monomers, and r_0 is the critical distance, below which the neck linker is unstretched. Note that, in the present system, the stepping dynamics of the walker is independent of values of the internal elastic force C and the critical length r_0, provided that r_0 is slightly smaller than the period d of the binding sites along the track.

The interaction between the monomer and track can also be considered to be via electrostatic force, which is dependent on the charge distributions on the two binding surfaces. Thus, the monomer binds the binding site of the track in a fixed orientation, as shown in Fig. 1(b). The interaction potential between the monomer and track can be written in the form

$$V_S(x,y,z) = V_S^{(x)}(x)\exp[-(y-y_0)/A_y]\exp[-|z-z_0|/A_z] \quad (y \geqslant y_0). \quad (3)$$

Here $V_S^{(x)}(x) \leqslant 0$ (with the maxima equal to zero) represents the periodic potential along the track or along the longitudinal (x) direction and is schematically shown in Fig. 1(c), where E_0 is the depth of the potential well; y_0 and z_0 are the coordinates of the binding site on the track along the vertical (y) and horizontal (z) directions, respectively. Note that either a symmetric or an asymmetric form of $V_S^{(x)}(x)$ is applicable to the system except the requirement of a fixed binding orientation of the monomer relative to the track at the minimum of the potential well. Terms $\exp[-(y-y_0)/A_y]$ and $\exp[-|z-z_0|/A_z]$ denote the potential change in the vertical and horizontal directions, respectively, with A_y and A_z characterizing the Debye lengths. To realize the unidirectional movement, it is required that a technical means or an external operation can transiently weaken the binding affinity of the monomer to the track. Here we adopt the following design. Only the track-binding affinity of the monomer whose neck liner is docked into the domain or the monomer that is pulled forwards by the neck linker [e.g., the left monomer in Fig. 1(b)] can be transiently weakened by the external operation. The transient weak interaction potential induced by the external operation $V_W(x,y,z)=\text{const}$ lasts a time of t_0. The external operation has no effect on the track-binding affinity of the monomer whose neck liner is undocked into the domain or the monomer that is pulled backwards by the neck linker [e.g., the right monomer in Fig. 1(b)].

With one monomer bound strongly to the track at position $(x,y,z)=(0,0,0)$, the temporal evolution of the center-of-mass position of the other monomer (relative to that of the first one) after an external operation satisfies the following Langevin equations:

$$\Gamma\frac{\partial x}{\partial t} = -\frac{\partial V_T(x,y,z)}{\partial x} - \frac{\partial V_{M-M}(x,y,z)}{\partial x} - F_{NL}(r)\frac{x}{r} - F_{load}/2 + \xi_x(t), \quad (4a)$$

$$\Gamma\frac{\partial y}{\partial t} = -\frac{\partial V_T(x,y,z)}{\partial y} - \frac{\partial V_{M-M}(x,y,z)}{\partial y} - F_{NL}(r)\frac{y}{r} + \xi_y(t), \quad (4b)$$

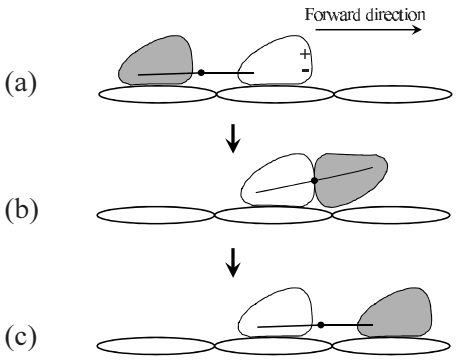

FIG. 2. Schematic illustrations of the unidirectional movement of the homodimeric nanowalker. For clarity, the two identical monomers are shown in gray and white. (a) The stepping cycle begins with both monomers binding to the track. (b) An external operation transiently weakens the track-binding affinity of the trailing monomer (gray) whose neck linker is docked (or the monomer that is pulled forwards by the neck linker). The gray monomer then diffuses to the position where it has the strongest interaction with another monomer (white) that is bound strongly to the track. (c) After the track-binding affinity of the gray monomer is resumed, it binds to the nearest binding site of the track due to the larger track-binding affinity than the binding affinity between the two monomers. From (a) to (c), a forward step has been made.

$$\Gamma\frac{\partial z}{\partial t} = -\frac{\partial V_T(x,y,z)}{\partial z} - \frac{\partial V_{M-M}(x,y,z)}{\partial z} - F_{NL}(r)\frac{z}{r} + \xi_z(t), \tag{4c}$$

where $V_T(x,y,z)=V_W(x,y,z)$ when $t_0<0$ and $V_T(x,y,z)=V_S(x,y,z)$ when $t_0\geqslant 0$. F_{load} is the backward load acting on the dimer via their neck linkers. Here, we consider that half of F_{load} is acting on the moving monomer while the other half is acting on another monomer, and this splitting is independent of the relative position of the monomers [38]. Approximating the monomer as a sphere of radius R, due to the steric restriction of the track, it is required that $y\geqslant y_0=0$ and $r\geqslant 2R$. Here, the drag coefficient is $\Gamma=6\pi\eta R$, where η is the viscosity of the aqueous medium. As the viscosity of the aqueous cytoplasm does not differ from water [39], we take $\eta=0.01$ g cm^{-1} s^{-1}. $\xi_m(t)$ $(m=x,y,z)$ is the fluctuating Langevin force, with $\langle\xi_m(t)\rangle=0$ and $\langle\xi_m(t)\xi_n(t')\rangle=2k_BT\cdot\Gamma\cdot\delta_{mn}\delta(t-t')$, where k_B is the Boltzmann constant and $T=300$ K.

III. RESULTS

The unidirectional movement of the nanowalker along the track is schematically illustrated in Fig. 2. Next we quantitatively study the stepping dynamics.

Equation (4) is solved numerically by using the stochastic Runge-Kutta algorithm [40]. For the calculation, the period of the binding sites along the track is taken to be $d=10$ nm and the radius of the monomer is taken to be $R=3$ nm. Since inside the cell the Debye length is in the order of 1 nm, we take $A_r=A_y=A_z=1$ nm. Moreover, it has been checked that, by taking $A_r=A_y=A_z=0.5$ nm or taking $A_r=A_y=A_z=2$ nm, we obtained the same statistical results for the stepping dynamics. As it is required that E_0 is larger than V_0, we take $V_0=15k_BT$ and $E_0=30k_BT$ in the calculation. Moreover, it has been checked that, by taking $(V_0,E_0)=(20k_BT,30k_BT)$ or $(V_0,E_0)=(12.5k_BT,25k_BT)$ or $(V_0,E_0)=(15k_BT,25k_BT)$, we obtained the same statistical results. The stepping dynamics of the walker should be independent of values of the internal elastic force C and the critical length r_0, provided that r_0 is slightly smaller than the value of d. For the calculation, we take $r_0=9$ nm and $C=5$ pN/nm. Since the stepping dynamics is sensitively dependent on the value of t_0, we take it as a variable parameter.

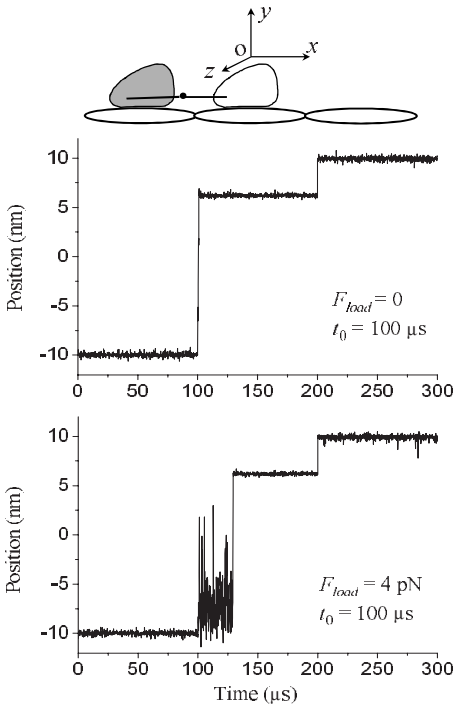

FIG. 3. Results for the temporal evolution of the position of the gray monomer relative to the white one bound strongly to the track at position (0,0,0) under the external load F_{load}. The external operation that interacts with the gray monomer occurs at $t=100$ μs and the transient weak potential induced by the external operation lasts $t_0=100$ μs. For clarity, only the results for the x component are shown here. The top figure shows schematically the positions of the two monomers before the external operation.

In Fig. 3 we show two typical results for the temporal evolution of the position of the gray monomer relative to the white one bound strongly to the track at position (0,0,0) (see the top figure in Fig. 3). Here, it is taken that an external operation occurs at $t=100$ μs and the transient weak potential induced by the external operation lasts $t_0=100$ μs. It is seen that, as anticipated, the walker steps forwards in the hand-over-hand manner and one step consists of two substeps. During the first substep, the detached gray monomer moves from the trailing position at $(-10\text{ nm},0,0)$ [as schematically shown in Fig. 2(a)] to the leading position at $(6\text{ nm},0,0)$ [as schematically shown in Fig. 2(b)] where the two monomers have the strongest interaction. During the second substep, the detached monomer moves from the position at $(6\text{ nm},0,0)$ to that at $(10\text{ nm},0,0)$ [as schematically shown in Fig. 2(c)] after the interaction between the detached

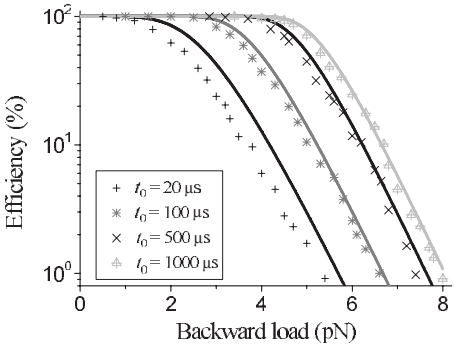

FIG. 4. Results of the efficiency ε versus backward load F_{load} for different values of t_0. Lines represent the analytical results from Eqs.(5) and (6) and symbols represent the statistical results calculated numerically using Eq. (4).

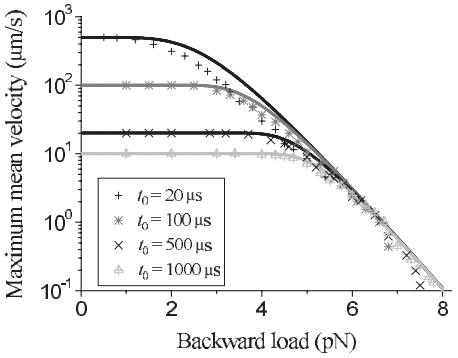

FIG. 5. Results of the maximum mean velocity that the walker can attain versus backward load F_{load} for different values of t_0. Lines represent the analytical results and symbols represent the numerical results. The results are obtained by using $V=\varepsilon d/t_0$, with ε from Fig. 4.

gray monomer and the track is resumed to its normal strong value. The first substep is realized mainly by the Brownian motion, while the second substep is mainly driven by the strong interaction between the detached monomer and its nearest binding site on the track. Thus, the time to make the first substep is approximately equal to the fist-passage time of the Brownian particle diffusing from position at $(-10\ \text{nm},0,0)$ to that at $(6\ \text{nm},0,0)$. As a result, under low backward loads, the time of the first substep is short, while under large backward loads, the time is long. However, during the second substep, due to the large forward driving force from the track, the stepping time is short even under large backward loads.

To see the efficiency of the walker, in Fig. 4 we show the statistical results (denoted by symbols) of the efficiency, $\varepsilon \equiv N_{step}/N_{input}$, versus backward load F_{load} for different values of t_0. Here, N_{step} is the number of effective stepping [i.e., one monomer moving from the position at $(-10\ \text{nm},0,0)$ to that at $(10\ \text{nm},0,0)$ after the occurrence of an external operation] and N_{input} is the total number of external operations. In this system, N_{step} is actually equal to the occurrence number that the trailing monomer moves to the leading position at $(6\ \text{nm},0,0)$, where the two monomers have the maximum interaction. This is because, after the detached monomer moves to the position at $(6\ \text{nm},0,0)$, it will move to the position at $(10\ \text{nm},0,0)$ with an efficiency of 100% when its strong interaction with the track is resumed. Thus, we can use the following procedure to approximately calculate ε analytically. As mentioned above, the time to make the first substep is approximately equal to the fist-passage time T_{FP} of the Brownian particle diffusing from position at $(-10\ \text{nm},0,0)$ to that at $(6\ \text{nm},0,0)$. The mean value of T_{FP} can be calculated by

$$\langle T_{FP}\rangle = \frac{1}{f}\left\{\frac{D}{f}\left[\exp\left(\frac{f}{D}L\right)-1\right]-L\right\}, \tag{5}$$

where $f=F_{load}/(2\Gamma)$, $D=k_BT/\Gamma$, and $L=16$ nm. As shown in Ref. [41], a good approximation to the distribution of T_{FP} is given by $g(t)=(1/\langle T_{FP}\rangle)\exp(-t/\langle T_{FP}\rangle)$. As a result, the efficiency can be calculated by $\varepsilon=\int_0^{t_0} g(t)dt$, which has the form

$$\varepsilon = 1-\exp(-t_0/\langle T_{FP}\rangle). \tag{6}$$

Using Eqs. (5) and (6), the analytical results of ε versus F_{load} for different values of t_0 are shown by solid lines in Fig. 4. It is seen that, the numerical results are close to the approximate analytical results, especially for large values of t_0. From Fig. 4, it is interesting to note that, for $t_0=1$ ms, the efficiency is kept nearly 100% even for the backward load up to 4.5 pN. For $F_{load}>6$ pN, the efficiency decreases nearly exponentially with the increase of the backward load. If we define the stall force corresponding to the value at which the efficiency is equal to 1%, it is seen that, for $t_0=1$ ms, the stall force is about 8 pN. Even for $t_0=20$ μs, the stall force is still about 5.5 pN. Thus, the walker can move processively with a high efficiency and can exert a high stall force.

The maximum mean velocity that the walker can attain can be calculated by $V=\varepsilon d/t_0$. Using this equation and the results of ε versus F_{load} given in Fig. 4, we show V versus F_{load} for different values of t_0 in Fig. 5. It is seen that the walker can attain a very high velocity under low loads. For example, for $t_0=100$ μs, the maximum mean velocity is $V=100$ μm/s, and even for $t_0=1000$ μs, $V=10$ μm/s. These mean velocities are much larger than that of the wild-type kinesin-1, which is about 0.8 μm/s [27]. From Figs. 4 and 5, it is seen that, in order to have a high stall force or a wide range of F_{load} that can maintain nearly 100% efficiency, one should use a large value of t_0, whereas in order to have a large moving velocity, one should use a small value of t_0. Thus, in real design, one should choose an optimal value of t_0 to meet both the demand of high stall force and high efficiency and the demand of high velocity.

IV. DISCUSSION

In this work, we present a simple homodimeric nanowalker capable of walking processively along the periodic track. The interaction between the two monomers rather than the docking of the neck linker plays the critical role in the forward stepping of the detached trailing monomer. Besides the fundamental requirement of the interaction between the monomer and the track, the system has two other require-

ments. The first one is the interaction between two monomers. The other one is that the external operation only has an effect on the monomer whose neck liner is docked into the domain or the monomer that is pulled forwards by the neck linker, thus leading to the transient weakening of the binding affinity of the trailing monomer for the track. In other words, the external operation is required to have a much higher probability to weaken the track-binding affinity of the trailing monomer whose neck liner is docked (or the monomer that is pulled forwards by the neck linker) than the leading one whose neck linker is undocked (or the monomer that is pulled backwards by the neck linker). However, as we will discuss below, this requirement can be alleviated.

It is noted that, if an erroneous external operation transiently weakens the track-binding affinity of the leading monomer instead of that of the trailing one, the walker makes no stepping rather than a backward stepping, implying a futile operation. This can be seen in Fig. 6, where we show a typical numerical result for the temporal evolution of the white monomer relative to the gray one bound strongly to the track at position (0,0,0) (see the top figure in Fig. 6). Here it is taken that the external operation occurs at $t=100$ μs and the transient weak potential induced by the external operation lasts $t_0=100$ μs. As a result, if the external operation has a probability of p to weaken the track-binding affinity of the monomer whose neck liner is docked, the efficiency of the walker becomes $\varepsilon'=p\varepsilon$, where ε is shown in Fig. 4 for $p=1$. In particular, even if the external operation has the same probability to weaken the track-binding affinity of either of two monomers, the walker can still make the unidirectional movement, but with the efficiency being replaced by $\varepsilon'=\varepsilon/2$. In other words, if the external operation has no discriminative effect on the two monomers, the walker can still walk processively along the track, provided that an operation only has the effect on one monomer.

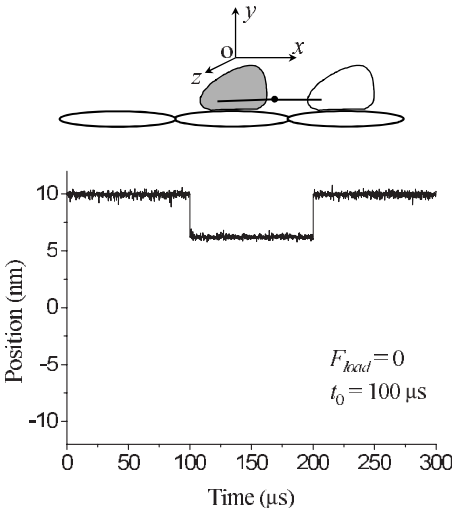

FIG. 6. Results for the temporal evolution of the position of the white monomer relative to the gray one bound strongly to the track at position (0,0,0) under $F_{load}=0$. The external operation that interacts with the white monomer occurs at $t=100$ μs and the transient weak potential induced by the external operation lasts $t_0=100$ μs. For clarity, only the results for the x component are shown here. The top figure shows schematically the positions of the two monomers before the external operation.

V. CONCLUSION

We showed that a homodimeric nanowalker can walk unidirectionally along an extended periodic track by making use of the interaction between the two monomers and the thermal noise. The effect of the neck linker, which plays a critical role for the unidirectional movement of the homodimer in the previously proposed design, plays an unimportant role in the present system. Except the requirement of a fixed binding orientation of the monomer relative to the track at the minimum of the potential well, the system has no other requirement for the form of the potential of the motor interacting with the track, which is critical to the unidirectional movement of the monomeric motor. Detailed calculations show, however, that the dimeric nanowalker can walk hand-over-hand along the periodic track with a high efficiency, a high velocity, and a high stall force.

ACKNOWLEDGMENTS

The author is grateful to the reviewer's helpful comments. This work is supported by the National Basic Research Program of China (973 Program) (Grant No. 2009CB930704).

[1] R. A. Bissell, E. Cordova, A. E. Kaifer, and J. F. Stoddart, Nature (London) **369**, 133 (1994).
[2] T. R. Kelly, H. De Silva, and R. A. Silva, Nature (London) **401**, 150 (1999).
[3] N. Koumura, R. W. J. Zijlstra, R. A. van Delden, N. Harada, and B. L. Feringa, Nature (London) **401**, 152 (1999).
[4] B. Yurke, A. J. Turberfield, A. P. Mills, F. C. Simmel, and J. L. Neumann, Nature (London) **406**, 605 (2000).
[5] A. M. Brouwer, C. Frochot, F. G. Gatti, D. A. Leigh, L. Mottier, F. Paolucci, S. Roffia, and G. W. H. Wurpel, Science **291**, 2124 (2001).
[6] D. A. Leigh, J. K. Y. Wong, F. Dehez, and F. Zerbetto, Nature (London) **424**, 174 (2003).
[7] J. D. Badjic, V. Balzani, A. Credi, S. Silvi, and J. F. Stoddart, Science **303**, 1845 (2004).
[8] J. V. Hernandez, E. R. Kay, and D. A. Leigh, Science **306**, 1532 (2004).
[9] S. P. Fletcher, F. Dumur, M. M. Pollard, and B. L. Feringa, Science **310**, 80 (2005).
[10] T. Muraoka, K. Kinbara, and T. Aida, Nature (London) **440**, 512 (2006).
[11] R. D. Astumian, Science **276**, 917 (1997).
[12] F. Jülicher, A. Ajdari, and J. Prost, Rev. Mod. Phys. **69**, 1269 (1997).

[13] J. Rousselet, L. Salome, A. Ajdari, and J. Prost, Nature (London) **370**, 446 (1994).
[14] W. B. Sherman and N. C. Seeman, Nano Lett. **4**, 1203 (2004).
[15] J. S. Shin and N. A. Pierce, J. Am. Chem. Soc. **126**, 10834 (2004).
[16] P. Yin, H. Yan, X. G. Daniell, A. J. Tuerberfield, and J. H. Reif, Angew. Chem., Int. Ed. **43**, 4906 (2004).
[17] J. Bath, S. J. Green, and A. J. Turberfield, Angew. Chem., Int. Ed. **44**, 4358 (2005).
[18] Y. Tian, Y. He, Y. Chen, P. Yin, and C. Mao, Angew. Chem., Int. Ed. **44**, 4355 (2005).
[19] J. Berna, D. A. Leigh, M. Lubomska, S. M. Mendoza, E. M. Perez, P. Rudolf, G. Teoberto, and F. Zerbetto, Nature Mater. **4**, 704 (2005).
[20] Y. Shirai, A. J. Osgood, Y. Zhao, K. F. Kelly, and J. M. Tour, Nano Lett. **5**, 2330 (2005).
[21] M. O. Magnasco, Phys. Rev. Lett. **71**, 1477 (1993).
[22] R. Bartussek, P. Reimann, and P. Hanggi, Phys. Rev. Lett. **76**, 1166 (1996).
[23] P. Jung, J. G. Kissner, P. Hanggi, and M. Nagaoka, Phys. Rev. Lett. **76**, 3436 (1996).
[24] R. D. Astumian and M. Bier, Phys. Rev. Lett. **72**, 1766 (1994).
[25] J. Prost, J.-F. Chauwin, L. Peliti, and A. Ajdari, Phys. Rev. Lett. **72**, 2652 (1994).
[26] R. D. Vale, Cell **112**, 467 (2003).
[27] K. Visscher, M. J. Schnitzer, and S. M. Block, Nature (London) **400**, 184 (1999).
[28] A. Yildiz, M. Tomishige, R. D. Vale, and P. R. Selvin, Science **303**, 676 (2004).
[29] R. D. Astumian and I. Derenyi, Biophys. J. **77**, 993 (1999).
[30] S. Klumpp, A. Mielke, and C. Wald, Phys. Rev. E **63**, 031914 (2001).
[31] Z. Wang, Proc. Natl. Acad. Sci. U.S.A. **104**, 17921 (2007).
[32] R. D. Vale and R. A. Milligan, Science **288**, 88 (2000).
[33] Z. Wang, M. Feng, W. Zheng, and D. Fan, Biophys. J. **93**, 3363 (2007).
[34] P. Xie, Biochim. Biophys. Acta **1777**, 1195 (2008).
[35] P. Xie, S.-X. Dou, and P.-Y. Wang, BioSystems **84**, 24 (2006).
[36] P. Xie, S.-X. Dou, and P.-Y. Wang, Biophys. Chem. **123**, 58 (2006).
[37] P. Xie, S.-X. Dou, and P.-Y. Wang, J. Mol. Biol. **366**, 976 (2007).
[38] The splitting of F_{load} among the two monomers could be dynamic in nature and it is rather difficult to give a precise and quantitative description of this splitting. The two limiting cases are one where the 50% splitting of F_{load} among the two monomers is independent of the relative position of the monomers, as discussed in the text, and one where F_{load} is always acting on the monomer when it is leading. For the latter limiting case, with both numerical simulation and approximate analytical study, we obtained a higher stall force and a wider range of F_{load} that can maintain nearly 100% efficiency than for the former limiting case. For example, when $t_0=1$ ms, the stall force is about 8 pN for the former limiting case (see Fig. 4), while it is about 11.9 pN for the latter case. In a real situation, the splitting of F_{load} among the two monomers should always be in between the two limiting cases. Thus, the stall forces and efficiencies presented in the text are the most conservative values that our proposed walker can attain.
[39] K. Luby-Phelps, S. Mujumdar, R. B. Mujumdar, L. A. Ernst, W. Galbraith, and A. S. Waggoner, Biophys. J. **65**, 236 (1993).
[40] R. L. Honeycutt, Phys. Rev. A **45**, 600 (1992).
[41] R. F. Fox and M. H. Choi, Phys. Rev. E **63**, 051901 (2001).